Disturbance Triggers Non-Linear Microbe-Environment Feedbacks

Aditi Sengupta[1†], Sarah J. Fansler[2†], Rosalie K. Chu[3], Robert E. Danczak[2], Vanessa A. Garayburu-Caruso[2], Lupita Renteria[2], Hyun-Seob Song[4], Jason Toyoda[3], Jacqueline Wells[5], and James C. Stegen[2*]

[†]Denotes equal contribution

[1]California Lutheran University, Thousand Oaks, CA

[2]Pacific Northwest National Laboratory, Ecosystem Science Team, Richland, WA

[3]Environmental Molecular Sciences Laboratory, Richland, WA

[4]University of Nebraska-Lincoln, Lincoln, NE

[5]Oregon State University, Corvallis, OR

Correspondence to: James Stegen (James.Stegen@pnnl.gov)

Abstract

Conceptual frameworks linking microbial community membership, properties, and processes with the environment and emergent function have been proposed but remain untested. Here we refine and test a recent conceptual framework using hyporheic zone sediments exposed to wetting/drying transitions. Our refined framework includes relationships between cumulative properties of a microbial community (*e.g.* microbial membership, community assembly properties, and biogeochemical rates), environmental features (*e.g.* organic matter thermodynamics), and emergent ecosystem function. Our primary aim was to evaluate the hypothesized relationships that comprise the conceptual framework and contrast outcomes from the whole and putatively active bacterial and archaeal communities. Throughout the system we found threshold-like responses to the duration of desiccation. Membership of the putatively active bacterial community--but not the whole bacterial and archaeal community--responded due to enhanced deterministic selection (an emergent community property). Concurrently, the thermodynamic properties of organic matter (OM) became less favorable for oxidation (an environmental component) and respiration decreased (a microbial process). While these responses were step functions of desiccation, we found that in deterministically assembled active communities, respiration was lower and thermodynamic properties of OM were less favorable. Placing the results in context of our conceptual framework points to previously

27 unrecognized internal feedbacks that are initiated by disturbance, mediated by thermodynamics, and that

28 cause the impacts of disturbance to be dependent on the history of disturbance.

1 Introduction

1.1 Conceptual Foundations

32 Given the influence of microbes over ecosystem function, deeper knowledge of microbe-environment

33 relationships is needed to improve ecosystem models (Bier et al., 2015). In turn, there is strong interest

34 in quantifying and predicting microbe-environment relationships such as defining microbial life history

35 strategies as traits in ecosystem models (Malik et al., 2020), assessing microbial biomass stoichiometry

36 distributions in response to changing resource environments (Manzella et al., 2019), and evaluating the

37 extent of microbial adaptation to changing environments and their role in biogeochemical processes

38 (Wallenstein and Hall, 2012). To enhance and synthesize understanding of microbe-environment

39 interactions, it is useful to develop conceptual frameworks based on linkages among microbial

40 characteristics and ecosystem processes. Previous work has used such frameworks to improve

41 mechanistic representation and predictive capacity of microbe-environment interactions in ecosystem

42 models (Wieder et al., 2015).

44 A recently developed framework by Hall et al. (2018) poses a series of concepts that collectively define

45 the intersection between microbial and ecosystem ecology. Their framework draws attention to causal

46 relationships between microbial characteristics (microbial membership influences community properties

47 and microbial processes), which in turn regulate ecosystem fluxes. These components can be further

48 modified by environmental variation leading to cumulative ecosystems processes with the potential to

49 incorporate relevant mechanistic links into predictive ecosystem models. Hall et al. (2018) particularly

draws attention to the need to understand how microorganisms influence their environment by separating microbial community properties based on community aggregated traits (those which can be predicted using constituent taxa) and emergent properties (properties unable to be explained by constituent taxa). A powerful element of the framework is that it applies to diverse systems spanning natural (Gilbert et al., 2018), host-associated (Lloyd-Price et al., 2019), and built (Fu et al., 2020) environments as well as across spatiotemporal scales (König et al., 2018). While potentially very useful, the Hall et al. (2018) framework has seen little direct use in terms of explicitly defining and evaluating the linkages within specific study systems (but see Manzella et al., 2019). To make full use of and continually improve the framework, it is necessary to consider different realizations and interpretations of the proposed linkages. In the following paragraphs we detail a modified interpretation of the framework (**Fig. 1**) to enable its application to microbial communities and biogeochemistry associated with hyporheic zone sediments experiencing hydrological disturbance. In turn, we use data from a controlled laboratory experiment to evaluate key linkages within the modified framework.

Our modified framework aims to refine the link between microbial communities and ecosystem functions. As detailed below, a couple critical elements of our modification include: Defining and evaluating the relative influence of community assembly processes as an emergent community property, and ii) proposing bi-directional links between environment and microbial processes to indicate that environmental conditions drive microbial processes, which in turn influence the environment, and these cumulative environment-microbial processes ultimately drive ecosystem function.

1.2 Conceptual Framework Development

73   As in Hall et al. (2018) we consider microbial membership to be directly influenced by environmental

74   conditions (arrow 4, Fig.1) and to underlie community-level properties (arrow 1, Fig. 1). Determining

75   microbial membership is relatively straightforward, and uses culture-independent (Behrens et al., 2012;

76   Norland et al., 1995; Thompson et al., 2017; Wagner, 2009) and culture-dependent (Bartelme et al.,

77   2020) techniques. Sequence-based assays using phylogenetic markers are routine, with DNA-based

78   (total community members) and RNA-based (putatively active community members) (Barnard et al.,

79   2015; Blazewicz et al., 2013; Cardoso et al., 2017; Kearns et al., 2016; Shu et al., 2019; Wisnoski et al.,

80   2020) approaches providing the foundation to study community properties.

81

82   While community membership is relatively straightforward, the identification of community properties

83   that are relevant to a given system and function is open to broader interpretation. Here we propose using

84   the relative influences of deterministic and stochastic community assembly processes (Stegen et al.,

85   2012) as emergent properties of microbial communities that have implications for biogeochemical

86   function (Graham and Stegen, 2017) including in ecosystems experiencing environmental disturbance.

87   Deterministic mechanisms are associated with systematic differences in reproductive success imposed

88   by the biotic and/or abiotic environment, while stochastic mechanisms are associated with passive

89   spatial movements of organisms and birth/death events that are not due to systematic differences across

90   taxa in reproductive success (Dini-Andreote et al., 2015; Stegen et al., 2015). The relative contributions

91   of determinism and stochasticity can be inferred by coupling microbial community membership and

92   phylogeny to ecological null models (Stegen et al., 2012, 2013, 2015; Zhou and Ning, 2017).

93

94   We propose that the relative contributions of determinism and stochasticity are emergent properties that

95   are greater than the sum of the individual components (i.e., taxa), and that are complementary to the

96   community properties proposed by Hall et al. (Hall et al., 2018), such as biomass and gene expression.

97   Furthermore, we propose that there are feedbacks between assembly processes and microbial

98   membership whereby assembly processes influence which taxa are found in which abundances, but

99   biotic interactions also influence assembly processes. In turn, we modified the framework whereby

100   arrow 1 is bidirectional (Fig. 1).

101

102   It is important to recognize that the ecological processes of community assembly are distinct from

103   'microbial processes' associated with biogeochemical reactions. As an emergent property, the relative

104   influence of determinism and stochasticity is the result of complex biotic and abiotic interactions (Grilli

105   et al., 2017) and also shapes cumulative microbial processes that impact ecosystem biogeochemical

106   functions (Graham and Stegen, 2017) (arrow 2, Fig.1). For example, a stronger influence of determinism

107   over community assembly is hypothesized to cause higher respiration rates (a microbial processes) due

108   to a larger contribution of well-adapted taxa (Graham and Stegen, 2017), though the respiration response

109   may vary depending on the existing community composition and the deterministic forces exerted.

110

111   Analyses of microbial community assembly have been widely employed across environments including

112   soil (Bottos et al., 2018; Dini-Andreote et al., 2015; Feng et al., 2018; Jurburg et al., 2017; Sengupta et

113   al., 2019b), sediment (Graham et al., 2017a; Stegen et al., 2013, 2016, 2018b), marine (Starnawski et al.,

114   2017; Wu et al., 2018), riverine (Chen et al., 2019), gut (Martínez et al., 2015), and engineered (Ofiţeru

115   et al., 2010; Zhou et al., 2013) systems. Previous work has focused primarily on using DNA-derived

116   membership and phylogenetic data to study whole-community assembly. In contrast, recent studies have

117   also used an RNA-based approach to study the relative influence of stochasticity over the assembly of

118   the putatively active portion of microbial communities (Jia et al., 2020; Jurburg et al., 2017). This RNA-

119   based approach is complementary to the DNA-based approach and may provide additional insights into

120   shorter-term dynamic linkages between emergent community properties and microbial processes. Such

121   linkages have not, however, been previously evaluated.

122

123   The Hall et al. (2018) framework proposes that microbial processes (e.g., respiration rate) are

124   influenced by both microbial community properties and environmental factors. Here we propose a

125   revision of this structure that includes bidirectional links between the environment and microbial

126   processes (arrow 3, Fig. 1). Such bi-directional links between microbes and their environment are

127   common (Daly et al., 2016; Leventhal et al., 2019; Ratzke et al., 2018; Stegen et al., 2018a), and in

128   hyporheic zone sediments may be particularly tied to thermodynamic properties of organic matter

129   (Graham et al., 2018) and influenced by hydrological disturbances that are common in such

130   environments. For example, preferential use of OM by microbial communities has potential to alter the

131   thermodynamic properties of organic matter pools (Graham et al., 2017a). This microbe-driven shift in

132   the environment could then feedback to impact microbial metabolism due to the strong influence of OM

133   thermodynamics on biogeochemical rates (Boye et al., 2017; Garayburu-Caruso et al., 2020; Song et al.,

134   2020; Stegen et al., 2018b). Bi-directional feedback between environmental factors and microbial

135   processes is, therefore, likely important to the link between microbial communities and ecosystem

136   function. Fundamental knowledge of these feedbacks and how they are modulated by hydrologic

137   disturbances in hyporheic zone sediments is largely unknown, however.

138

139   Within ecosystems, mechanistic associations between environmental factors, microbial properties, and

140   microbial processes underlie spatial and temporal distributions of biogeochemical rates (Fig. 1 arrow 5).

141   The resulting distributions (e.g., of respiration rates) define cumulative system function and can be used

142   to understand key phenomena such as biogeochemical hot spots and hot moments (McClain et al.,

143   2003). Developing concepts and models to predict the influences of biogeochemical hot spots/moments

144   is a major outstanding challenge. To facilitate progress, Bernhardt et al. (2017) proposed grouping hot

145   spots/moments into the concept of ecosystem control points that exert a disproportionate influence on

146   ecosystem function.

147

148   While not called out explicitly in Bernhardt et al. (2017), the control point concept is based on the

149   distribution of biogeochemical rates through space and/or time. Focusing on the shape of rate

150   distributions allows the notion of control points to be extended to the concept of control point influence

151   (CPI; Fig. 1 arrow 5). The CPI is a quantitative measurement of the contribution of elevated

152   biogeochemical rates in space and/or time to the net aggregated rate within a defined system (Arora et

153   al., 2020). While proposed conceptually and studied via simulation in Arora et al. (2020), empirical

154   measurements of CPI are lacking. More generally, incorporating CPI into a modified version of the Hall

155   et al. (2018) framework (Fig. 1), provides an integrated conceptualization for how environmental

156   factors, microbial properties, and microbial processes contribute to emergent system function.

157

158   Some elements of our modified framework (Fig. 1) are generalizable across systems (e.g., CPI), while

159   others (e.g., OM thermodynamics) may have different levels of relevance across different ecosystem

160   types. Here we aim to generate fundamental knowledge of the linkages between microbial community

161   and ecosystem function, as well as reveal how hydrologic disturbance may modify these linkages. While

162   relationships between microbial community assembly and function have been evaluated, integrating the

163   concepts of microbial structure, function, assembly, and environment interactions into one coherent

164   framework has the potential to advance our understanding of the feedbacks between microbial

165   communities and the environment.

166

167   1.3 Study Objectives

168   Our primary objective was to study the modified conceptual framework in context of variably inundated

169   hyporheic zone sediments exposed to different drying/wetting dynamics. Hyporheic zones are

170   biogeochemically active subsurface domains in river corridors through which surface water flows and

171   can mix with groundwater (Bernhardt et al., 2017; Boano et al., 2014; McClain et al., 2003). These

172   zones can have disproportionate biogeochemical impacts on river corridors (Boano et al., 2014; Burrows

173   et al., 2017; Demars, 2019; Fischer et al., 2005; Kaufman et al., 2017). Within variably inundated

174   streams (Larned et al., 2010; Romaní et al., 2006), hyporheic zones experience extreme changes in

175   environmental conditions, but the consequences of this variability for microbe-ecosystem linkages is

176   poorly known.

177

178   To mimic natural disturbances, we subjected sediments to wetting-drying transitions and focused on a

179   series of analyses tied to our modified framework. We specifically evaluated relationships between: (*i*)

180   the relative influence of stochastic assembly as a community property and respiration rates as a

181   microbial process (Fig. 1 arrow 2), and (*ii*) environmental features and both microbial properties (Fig. 1

182   arrow 4) and processes (Fig. 1 arrow 3) that underlie aggregate system function (Fig. 1 arrow 5). We

183   evaluated relationships between cumulative properties of the microbial community (membership,

184   assembly, biogeochemical rates), environmental features, and emergent ecosystem function by

185   hypothesizing that: (*i*) Stronger influences of determinism result in well-adapted microbes that will

186   generate higher respiration rates, (*ii*) Longer duration in an inundated state will result in greater

187   influences of stochastic assembly--due to weaker ecological selection--and lower respiration rates

188 following re-inundation due to relatively consistent abiotic conditions (Birch, 1964), (*iii*) Microbial

189 processes are facilitated by OM that is thermodynamically more favorable for oxidation, leading to an

190 association between respiration rates and OM thermodynamics, and (*iv*) More wet/dry transitions will

191 increase among-replicate heterogeneity (e.g., in microbial membership) thereby increasing CPI by

192 increasing within-treatment variability in respiration rates.

193

194 2 Methods

195 2.1 Study site and sediment collection

196 Hyporheic sediments were collected from the Columbia River shoreline (approximately 46.372411°N,

197 119.271695°W) in eastern Washington State (Fig S1) (Arntzen, 2006; Goldman et al., 2017; Graham et

198 al., 2016; Slater et al., 2010; Stegen et al., 2018b; Zachara et al., 2013) within the Hanford Site on

199 January 14, 2019 at 9 am Pacific Standard Time. Samples were aseptically collected to a depth of 10 cm

200 at five sub-sampling locations within a meter to form a composite sample that was sieved on site

201 through a 2 mm sieve into a clean glass beaker. Sieved sediment was stored on blue ice for 30 min while

202 being transported back to the laboratory. Once back at the laboratory sediment was stored at 4 °C until

203 processing into incubation vials (see below).

204

205 The sediments were subjected to increasing temporal environmental variance (as a function of periodic

206 wetting and drying transitions) and evaluated for associations between microbial membership, microbial

207 properties, microbial community assembly, OM chemistry, absolute respiration rate (represented in this

208 study as O_2 consumption rates), and cumulative respiration rates represented as CPI. Aerobic respiration

209 was chosen as the biogeochemical process since it influences global-scale energy and material fluxes

210   (Fatichi et al., 2019), and because the hyporheic zone within the field system is predominantly aerobic

211   (Graham et al., 2016, 2017b). Detailed experimental design and methods are provided in the following

212   paragraphs.

213

2.2 Experimental design

215   Sediments used in the batch reactors were sourced from one homogenized sediment pool. In turn, 10 g

216   of sediment from the homogenized pool was added to each reactor vial. The sample set was then split

217   into two groups, one inundated and the other allowed to desiccate. Desiccation was achieved within 15-

218   17 days. Sediments were periodically weighed to allow the inundated samples to be maintained at a

219   constant water content and to monitor the remaining samples for desiccation. Inundated sediments were

220   placed on ceramic porous plates saturated with DI water for weight adjustments. These conditions were

221   maintained for 23 days prior to the start of dynamic moisture manipulation, from January 29th to

222   February 21st, 2019. This initial 'preconditioning' period was used to avoid measuring the immediate

223   impacts of sampling disturbance and to allow time for desiccation. All replicate reactors were

224   maintained in the dark, shaking at 100 rpm, at 21 ºC and were covered with a gas permeable Breathe-

225   Easy (Milli-Pore Sigma, Burlington, MA) membrane that allowed for gas exchange and drying. After

226   the preconditioning period in which sediments were consistently inundated or allowed to continuously

227   desiccate, the transition regimes (**Fig. 2**) were applied to the reactors starting on February 22nd, 2019.

228   We refer to the time from Feb 22nd, 2019 onwards as the 'transitions period' for all treatments, even

229   though some did not experience transitions between being inundated and dry. Each treatment had 6-7

230   replicates (detailed below). These regimes were designed around the number of wet/dry transitions

231   experienced by sediments within a given treatment. Treatment regimes also caused variation in the

232   cumulative number of days sediments were in a drying state. We imposed six different experimental

233   treatment regimes (**Fig. 2**) as follows:

234   ● 0 Transitions and 0 days of desiccation: Sediments were maintained at field moisture conditions

235   for the preconditioning and transitions periods. This treatment had 6 replicates.

236   ● 1 Transition and 34 days of desiccation: Sediments were dry during the preconditioning and

237   transitions periods, and transitioned once to the field moisture level prior to respiration

238   estimation. This treatment had 6 replicates.

239   ● 2 Transitions and 4 days of desiccation: Sediments were held at field moisture levels for the

240   preconditioning period and then for the first 7 days of the transitions period, then transitioned to

241   a dried state for 4 days, and transitioned to field moisture conditions prior to respiration

242   estimation. This treatment had 7 replicates.

243   ● 3 Transitions and 31 days of desiccation: Sediments were dry during the preconditioning period

244   and the first 4 days of the transitions period, then transitioned to field moisture levels for three

245   days, then transitioned to 4 days in a dried state, and transitioned again to field moisture levels

246   prior to respiration estimation. This treatment had 7 replicates.

247   ● 4 Transitions and 8 days of desiccation: Sediments were held at field moisture levels for the

248   preconditioning period and transitioned to a dried state for the first 4 days of the transitions

249   period, then transitioned to field moisture levels for 3 days, then transitioned to 4 days in a dried

250   state, and transitioned to field moisture levels prior to respiration estimation. This treatment had

251   7 replicates.

252   ● 5 Transitions and 27 days of desiccation: Sediments were dry during the preconditioning period

253   and then transitioned to field moisture levels for the first 3 days of the transitions period,

254   transitioned to a dried state for 2 days, transitioned to field moisture levels for 2 days,

255   transitioned to a dried state for 2 days, and transitioned to field moisture levels for 3 days prior to

256   respiration estimation. This treatment had 7 replicates.

257

258   To avoid modifying electrical conductivity across experimental treatments, sterile deionized water was

259   added to reactors to achieve/maintain field moisture levels according to the defined wet/dry regimes

260   detailed above. For reactors with sediments that were below field moisture levels, deionized water was

261   added to achieve field moisture levels prior to respiration rate estimation. Changes in the total mass of

262   reactors and volumes of water added during the course of the experiment are provided in Table S1.

263

264 ## 2.3 Respiration rate measurements

265   Laboratory incubations were performed in batch reactors to quantify dissolved oxygen consumption

266   rates. Borosilicate glass vials (20 ml) (I-Chem™ Clear VOA Glass Vials, Thermo-Fisher, Waltham,

267   MA) served as incubator reactors. Factory calibrated oxygen sensor spots (Part# 200001875, diameter =

268   0.5 cm, detection limit 15 ppb, 0 – 100 % oxygen; PreSens GmbH, Regensburg, Germany) were adhered

269   to the inner vials of the reactor prior to sediment addition. Detailed description of sensor adhesion and

270   non-destructive measurements of DO consumption using these sensors is provided in Garayburo-Caruso

271   et al. (Garayburu-Caruso et al., 2020). Vials were grouped into six treatment regimes (explained in the

272   previous section) representing inundation-drought transitions.

273

274   Sample processing and incubations were performed in a laboratory at 21±1 °C. The reactors were

275   monitored for 2 hours, with measurement of dissolved oxygen (DO) concentration ($\mu mol\ L^{-1}$) every 30

276   min. DO concentration in each bioreactor was measured with an oxygen optical meter (Fibox 3;

277 PreSens GmbH) connected to a 2 mm polymer optical fiber lined up to sense the sensor dot every thirty

278 minutes. A few samples were discarded due to sensor dots detaching from the glass surface. Respiration

279 rates (μmol L^{-1} h^{-1}) were estimated as the slope of the linear regression between DO concentration and

280 incubation time for each sample. Some non-linearity was observed in the relationship between DO

281 concentration and time such that only the first 4 data points--time zero to 2 hours--were used to fit a

282 linear function. The slope of the linear function was taken as an estimate of respiration rate.

283

2.4 Microbial Analysis

285 Post-incubation, the sediment slurry was transferred to centrifuge tubes (Item#28-108 Genesee

286 Scientific) and centrifuged for 5 min at 3200 rcf and 20°C. The supernatant was removed and reserved

287 for biogeochemistry analyses and sediment aliquots for DNA and RNA extraction were flash-frozen in

288 liquid N$_2$ and stored at −80 °C. The extraction, purification, and sequencing of sediment microbial

289 gDNA were performed according to published protocol (Bottos et al., 2018). The extraction of RNA was

290 performed using the Qiagen PowerSoil RNA extraction kit (Qiagen, Germantown, MD). RNA was

291 treated with DNase and quantified with a Qubit RNA kit (Thermo Fisher, Waltham, MA). An aliquot of

292 the RNA extraction was used to generate cDNA using SuperScript™ IV First-Strand Synthesis System

293 (Thermo Fisher Scientific, Waltham, MA). The 16S rRNA gene sequencing--for both gDNA and

294 cDNA--followed the established protocol by The Earth Microbiome Project (Caporaso, 2018). Sequence

295 pre-processing, operational taxonomic unit (OTU) assignment, and phylogenetic tree building were

296 performed using an in-house pipeline, HUNDO (Brown et al., 2018). Sequences were deposited at

297 NCBI's Sequence Read Archive PRJNA641165. The final sample count of gDNA and cDNA,

298 respectively, for each treatment regime, after dropping samples following quality filtering and

299   rarefaction, was 5 and 5 (0 transition), 4 and 3 (1 transition), 5 and 4 (2 transitions), 7 and 6 (3

300   transitions), 7 and 6 (4 transitions), and 7 and 5 (5 transitions). Rarefaction levels are provided below in

301   the Statistics section.

302

2.5 Biogeochemistry

304   Reserved supernatant was filtered through a 0.22 μm polyethersulfone membrane filter (Millipore

305   Sterivex) and an aliquot was immediately removed for non-purgeable organic carbon (NPOC) and the

306   remainder was stored at -20C until further OM high resolution analysis was conducted (see below).

307   NPOC was determined by acidifying an aliquot of sample with 15% by volume of 2N ultra-pure HCL

308   (Optima grade, Fisher#A466-500). The acidified sample was sparged with carrier gas (zero air, Oxarc#

309   X32070) for 5 minutes to remove the inorganic carbon component. The sparged sample was then

310   injected into the TOC-L furnace of the Shimadzu combustion carbon analyzer TOC-L CSH/CSN E100V

311   with ASI-L auto sampler at 680°C using 150 uL injection volumes. The best 4 out of 5 injections

312   replicates were averaged to get the final result. The NPOC standard was made from potassium

313   hydrogen phthalate solid (Nacalia Tesque, lot M7M4380). The calibration range was 0 to 70 ppm

314   NPOC as carbon.

315   Fourier Transform Ion Cyclotron Resonance Mass Spectrometry (FTICR-MS) of post-incubation

316   sediment slurry was conducted as per Danczak et al. (2020). Sample processing, injection, and data

317   acquisition, processing and analysis was performed as per scripts provided in Danczak et al. (2020), with

318   'Start tolerance' in Formularity changed to 8. Ten samples were dropped due to poor calibration,

319   resulting in 5 replicates for 0 transition, 4 replicates for 1 transition, 5 replicates for 2 transitions, 6

320   replicates for 3 transitions, and 5 replicates each for 4 and 5 transition regimes.

321

322   From the FTICR-MS data, as in previous work (Garayburu-Caruso et al., 2020; Graham et al., 2018;

323   Sengupta et al., 2019b; Stegen et al., 2018b), we followed LaRowe and Van Cappellen (LaRowe and

324   Van Cappellen, 2011) to calculate the Gibbs free energy for the half reaction of organic carbon

325   oxidation under standard conditions (ΔG^0_{Cox}). This calculation is based on elemental stoichiometries

326   associated with molecular formulae assigned to individual molecules observed in the FTICR-MS data.

327   The formulae assignments are part of the processing scripts described in (Danczak et al., 2020). As in

328   previous work (Garayburu-Caruso et al., 2020; Graham et al., 2018; Sengupta et al., 2019b; Stegen et

329   al., 2018b), we interpret larger values of ΔG^0_{Cox} to indicate OM that is thermodynamically less favorable

330   for oxidation by microbes. That is, larger values of ΔG^0_{Cox} indicate OM that provides less net energy to a

331   microbial cell per oxidation event, assuming all else is equal. Given the large numbers of assigned

332   formulae within each sample, this resulted in thousands of ΔG^0_{Cox} estimates within each sample, from

333   which we estimated mean ΔG^0_{Cox} for each sample.

334

2.6 Estimating influences of community assembly processes

336   The relative influences of community assembly processes impacting microbial community membership

337   are emergent properties that cannot be calculated/inferred directly from knowledge of membership. To

338   evaluate assembly processes as a link between membership and microbial processes (refer Fig. 1) it is

339   necessary to quantitatively estimate the relative influences of these processes. To do so we use a well-

340   established null modeling framework based on phylogenetic relationships among microbial taxa (Dini-

341   Andreote et al., 2015; Stegen et al., 2012, 2015; Zhou and Ning, 2017). We refer the reader to these

342   previous studies for details. In brief, randomizations were used to generate estimates of phylogenetic

343   associations among microbial taxa for scenarios in which microbial communities were stochastically

344   assembled. These stochastic (i.e., null) expectations were compared quantitatively to observed

345   phylogenetic associations to estimate the β-Nearest Taxon Index (βNTI) (Stegen et al., 2012). We used

346   cDNA sequences rarefied to 27227 and gDNA sequences rarefied to 15106 sequences per sample to

347   determine putatively active community and whole community βNTI values, respectively. Samples

348   falling below these sequence counts were removed as indicated above in subsection *2.4 Microbial*

349   *Analysis.* A βNTI value of 0 indicates no deviation between the stochastic expectation and the observed

350   phylogenetic associations, thereby indicating the dominance of stochastic assembly processes. As βNTI

351   deviates further from 0, there is an increasing influence of deterministic assembly processes that drive

352   community membership away from the stochastic expectation. βNTI values below -2 or above +2

353   indicate statistical significance, with negative and positive values indicating less than or more than

354   expected shifts in membership. βNTI is a pairwise metric measured between any two

355   communities/samples, such that shifts in membership are related to changes between the pair of

356   communities being evaluated. We used βNTI to study all pairwise community comparisons within each

357   experimental treatment. Each community from a given reactor is therefore associated with multiple

358   βNTI values due to being compared to communities associated with other replicate reactors. In turn, the

359   average βNTI was calculated for each reactor. As in Stegen et al. (Stegen et al., 2015), this provides a

360   community-specific value for βNTI and thus an estimate of the relative influences of stochastic and

361   deterministic processes causing deviations between a given community and all other communities within

362   the same experimental conditions (Sengupta et al., 2019b). That is, the larger the absolute value of βNTI

363   for a given community, the stronger the influence of deterministic assembly processes acting on that

364   community (Stegen et al., 2015). In turn, these community-specific estimates were related to reactor-

365   specific measurements. For example, respiration rates were regressed against βNTI to evaluate the link

366   between emergent properties (i.e., ecological assembly) and microbial processes (i.e., respiration rates).

367

2.7 Evaluating relationships between microbial characteristics and environment

370   Respiration rate distributions, absolute βNTI values, and ΔG^0_{Cox} were summarized as box plots.

371   Pairwise Mann-Whitney test was performed to evaluate statistical differences between reactor-specific

372   measurements (*e.g.*,respiration rates and thermodynamic properties) and treatment groups (cumulative

373   dry and inundated days). Continuous bivariate relationships were evaluated with ordinary least squares

374   regression. Prior to regression analyses, respiration rates were log-transformed due to non-linearities

375   resulting from respiration being constrained to be at or above zero. Prior to log-transformation, half the

376   smallest non-zero rate was added to each rate to enable inclusion of rate estimates with a value of zero.

377

2.8 Control point influence calculation

379   To characterize respiration rate distributions we used the control point influence (CPI) metric. CPI was

380   recently developed (Arora et al., 2020) and is defined as the fraction of cumulative function (R_{tot}; e.g.,

381   total respiration rate) within a defined system that is contributed by individual rates that are above the

382   system's median rate (R_{med}). To define cumulative function one must first define the system being

383   evaluated. In our study, all replicate batch reactors within a given experimental treatment were

384   conceptualized as a representative set of samples from a larger system experiencing the experimental

385   conditions. R_{tot} for each treatment was therefore estimated as the sum of respiration rates across a

386   treatment's replicate reactors. CPI was estimated as the sum of respiration rates that fell above the

387   median rate for a given treatment (R_{above}) divided by R_{tot} for that treatment. That is, $R_{above} = \sum_{i}^{N} R_{i}$,

388   where R_i are respiration rates from individual reactors that fell above R_{med}, and $CPI = R_{above}/R_{tot}.$

389

390   An important feature of CPI is that it makes no assumptions of distribution normality, and can be

391   estimated for rate distributions of any form (e.g., unimodal, multimodal, Gaussian, skewed, etc.). In

392   most cases, CPI is constrained to have a minimum value of 0.5 (for a perfectly normal distribution with

393   no outliers) and asymptotically approach 1 as a maximum value (e.g., for heavily skewed distributions

394   with a small number of very high rates). CPI therefore quantitatively estimates the biogeochemical

395   contribution of places in space or points in time that have elevated biogeochemical rates.

396

397   Understanding how CPI varies through space, time, and with environmental conditions (e.g., disturbance

398   frequency) provides an opportunity to deepen our understanding of factors controlling hotspot/moment

399   behavior. Lower values of CPI (i.e., closer to 0.5) can arise through any mechanism that constrains

400   biogeochemical rates to be consistent through space or time. For example, if respiration rates were

401   measured in multiple locations across a well-mixed water body, we may expect a Gaussian rate

402   distribution with little variation. The cumulative respiration of the water body should not be influenced

403   significantly by hotspots, which would be reflected in low CPI. Conversely, higher values of CPI (i.e.,

404   closer to 1) can arise through any mechanism that increases the probability of positive outliers within a

405   given rate distribution. Spatial variation in the temporal dynamics of disturbances (e.g., more frequent

406   disturbances in some locations) is an example that is closely aligned with our experimental treatments.

407   In this case the probability of rate outliers (i.e., hotspots) may vary as a function of disturbance

408 frequency. For example, in spatial domains that experience more wetting/drying dynamics we might

409 expect a higher probability of rate outliers. This is because each time sediments go dry the exact spatial

410 distribution of water films that remain will vary across locations within the broader wetted/dried spatial

411 domain. In turn, we would expect higher values of CPI in spatial domains that are more frequently

412 wetted and dried. Regardless of whether this specific hypothesis is rejected or not, we contend that using

413 CPI enables development of *a priori* quantitative hypotheses spanning space, time, environmental

414 conditions (e.g., disturbance frequency), and scales. This provides new opportunities to more

415 systematically elucidate factors governing the influence of hotspots/moments.

3 Results

417 To link microbial membership to emergent microbial community properties (Fig. 1 arrow 1) we used

418 null modeling to estimate the contributions of stochastic and deterministic community assembly. Results

419 from the null models indicate a relatively balanced mixture of stochasticity and determinism for both the

420 whole community (gDNA-based) and putatively active community (rRNA-based) (Fig. S2). More

421 specifically, stochasticity and determinism each governed 50% of turnover in microbial membership for

422 the whole community and 33% and 67%, respectively, for the putatively active community. The relative

423 contributions of the two deterministic components (homogeneous and variable selection) were strongly

424 imbalanced. Homogeneous selection was responsible for 94% and 91% of the deterministic component

425 for the whole and putatively active communities, respectively. The contributions of homogeneous and

426 variable selection to the deterministic component must sum to 1, such that the variable selection was

427 responsible for 6% and 9% of the deterministic component for the whole and putatively active

428 communities, respectively.

429

430   As shown in Figure 1 (arrow 2), we hypothesized a link between microbial community properties and

431   microbial processes realized as a relationship between the strength of determinism and respiration rates.

432   Such a relationship was not observed for the whole community (Fig. 3a), but we did observe a non-

433   linear decreasing relationship between respiration rates and the absolute value of βNTI for the putatively

434   active community (Fig. 3b). The direction of this relationship (negative) was opposite of that expected,

435   and the relationship was clearly structured by among-treatment shifts in both respiration rate and βNTI

436   (Fig. 3b).

437

438   In our conceptual framework there are multiple ways in which connections among the environment,

439   microbial properties, and microbial processes may be realized, in part due to the environment having

440   multiple components relevant to our study (Fig. 1 arrows 3,4). More specifically, the environment was

441   characterized here in terms of both disturbance (number of dry days; imposed by the experimental

442   manipulation) and OM thermodynamics (ΔG^0_{Cox}; this is an emergent aspect of the environment).

443

444   Disturbance influenced both microbial properties and processes. These influences appeared to be non-

445   linear with experimental treatments associated with the two largest number of dry days (31 and 34)

446   causing decreases in respiration rates (Fig. 4a) and stronger influences of deterministic homogeneous

447   selection for the putatively active community (Fig. 4b). Disturbance had no clear influence on

448   community assembly for the whole community (Figs. S3, S4a). Given the apparent binary nature of

449   these results, we evaluated statistical significance by combining respiration rate data from treatments

450   with 0-27 cumulative dry days and separately combining data from treatments with 31 or 34 cumulative

451   dry days (Fig. S5). Respiration rates were significantly depressed in the treatments associated with 31 or

452   34 cumulative dry days ($W = 5$, $p < 0.001$). The βNTI data are non-independent due to being based on

453   all pairwise comparisons within a treatment. Standard statistical tools are therefore not applicable for

454   assigning statistical significance when comparing βNTI distributions. However, as shown in Figures 4b

455   and S4b, there is an obvious shift to lower βNTI values for the putatively active community in the

456   treatments with 31 or 34 cumulative dry days.

457

458   The other aspect of the environment examined here (i.e., OM thermodynamics) also had significant

459   relationships with both microbial processes (Fig. 1, arrow 3) and properties (Fig. 1, arrow 4). More

460   specifically, respiration rates decreased significantly as a negative exponential function of increasing

461   ΔG^0_{Cox} ($R^2 = 0.34$; $p = 0.001$; Fig. 5a). This indicates a decrease in respiration rate as OM

462   thermodynamic properties shifted towards lower favorability for oxidation (i.e., larger values of ΔG^0_{Cox}).

463   Similarly, we found that the strength of deterministic assembly associated with the putatively active

464   community increased linearly with ΔG^0_{Cox} ($R^2 = 0.40$; $p = 0.001$; Fig. 5b). The relationships were clearly

465   structured by among-treatment shifts in respiration rate, βNTI, and favorability of organic matter

466   (ΔG^0_{Cox}). The strength of deterministic assembly associated with the whole community was unrelated to

467   ΔG^0_{Cox} ($p = 0.64$) (Fig. S6).

468

469   The conceptual model described in Figure 1 focuses primarily on connections among environmental

470   and/or microbial attributes, but there are potentially important relationships within attribute categories.

471   In particular, within the environmental category there is the potential for an influence of disturbance on

472   OM thermodynamics. Such an effect was found for OM thermodynamics as measured by ΔG^0_{Cox} (Fig.

473   5c). Using the same approach as for analyses described above, we combined data for treatments with 0-

474   27 cumulative dry days and compared that distribution to data combined across treatments with 31 or 34

475   cumulative dry days. A Mann-Whitney test comparing these distributions confirmed a significant

476   change in the ΔG^0_{Cox} distribution (W = 189, p = < 0.001)(Fig. S7).

477

478   The last component of the conceptual model considered here is the connection between microbial

479   processes occurring in a given location and cumulative system function that aggregates across locations

480   (Fig. 1, arrow 5). It is at the system level that the influence of biogeochemical hot spots (or hot

481   moments) can be evaluated. We conceptualized an aggregate system as the collection of replicate batch

482   reactors within a given experimental treatment. Based on this definition, we estimated control point

483   influence (CPI) as a measurement for the influence of biogeochemical hot spots. We observed a large

484   amount of variation in CPI across experimental treatments, but there was no clear, direct influence of the

485   treatments on CPI (Fig. 4). The largest value of CPI observed (> 0.9) was associated with the treatment

486   that imposed 31 cumulative dry days. This treatment also had the lowest median respiration rates across

487   all treatments (Fig. 4). We did not find any significant relationship (p > 0.70) between within-treatment

488   community compositions (whole and putatively-active) and CPI, suggesting that within-treatment beta-

489   dispersion of the community is not a better predictor of CPI.

490

4 Discussion

492   Mechanistic evaluation of microbe-environment interactions is fundamental to understanding microbe-

493   mediated ecosystem function. Inspired by a microbe-environment-ecosystem framework proposed by

494   Hall et al. (Hall et al., 2018) we proposed and evaluated a modified framework linking microbial

495   characteristics (membership, emergent properties, processes), the environment (disturbance, OM

496   thermodynamics), and cumulative ecosystem function (CPI) of hyporheic zone sediments. Our results

497   provide clear support for the overall conceptual framework and further point to an iterative loop among

498   OM thermodynamics, respiration rates, and microbial community assembly that can be initiated by

499   externally-imposed disturbance. Furthermore, our results indicate that the iterative thermodynamics-

500   assembly-respiration loop may be initiated through threshold-like impacts of disturbance that were

501   observed only after 31 or more cumulative days of desiccation.

502

503   We first evaluated emergent community properties as a function of microbial membership by studying

504   the relative influences of stochasticity and determinism over community assembly. Taking this

505   approach, we found fully balanced stochastic-deterministic influences over the whole community, in

506   which each contributed to 50% of the variation in community composition. The relative influences of

507   stochasticity and determinism have been quantified for many microbial systems and the estimates are

508   highly variable (Tripathi et al., 2018; Wang et al., 2013). In addition, within the deterministic

509   component of assembly, homogeneous selection had a far greater influence than variable selection.

510   Previous work has also observed a broad range of contributions from homogeneous and variable

511   selection (Fillinger et al., 2019; Graham et al., 2016; Li et al., 2019; Sengupta et al., 2019a; Whitman et

512   al., 2018). As such, the assembly-associated outcomes observed here for the whole community are not

513   unexpected relative to previous work. Very few studies, however, have examined the relative influences

514   of different assembly components over putatively active microbial communities. This focus is critical in

515   our framework since many microorganisms are inactive while the active community remains sensitive to

516   abiotic stresses and contributes to ecosystem function.

517

518   For the putatively active communities we found that across all treatments both stochasticity and

519   determinism were important, though deterministic assembly had greater influence. This deviates

520   quantitatively from the whole community in which the influences of stochasticity and determinism were

521   more balanced. The difference in assembly influences in whole- and putatively-active communities is

522   likely driven by the duration of the imposed experimental treatments (two weeks). This time period may

523   not be sufficient for birth and death events to restructure the community composition. Instead,

524   physiological responses as a function of decreases and increases in microbial activity (changes in cDNA

525   signatures) is more likely. A stronger disturbance (*e.g.,* imposing the treatments for a longer period of

526   time) may provide further insights into the impacts of disturbance on the whole community (*e.g.,* evident

527   as changes in gDNA signatures). Consistent with the whole community results, however, was the

528   dominance of homogeneous selection within the deterministic component of assembly. The strong

529   influence of homogeneous selection is likely due to selection-based constraints imposed by aspects of

530   the experimental system that did not vary across treatments. For example, mineralogy is known to

531   strongly influence microbial communities (Boyd et al., 2007; Carson et al., 2009; Doetterl et al., 2018;

532   Fauvel et al., 2019; Mauck and Roberts, 2007; Stegen et al., 2016) and was homogenized across the

533   experimental batch reactors, thereby potentially imposing homogeneous selection on both the whole and

534   putatively active communities.

535

536   Our study uniquely evaluates null-model outcomes of putatively-active community assemblies in

537   hyporheic zone sediments, where homogeneous selection was further enhanced by our experimentally

538   imposed hydrologic disturbances. Increased homogeneous selection in response to disturbance is

539   consistent with previous work in aquatic (Chase, 2007) and soil systems. For example, in a soil system,

540   disturbance led to an immediate increase in homogeneous selection for the putatively active community

541   (Jurburg et al., 2017). The strong influence of homogeneous selection on the putatively active

542   community is not always observed, however, suggesting it may be tied to acute disturbance. That is, Jia

543   et al. (2020) recently found that within a natural soil chronosequence, variable selection was stronger for

544   putatively-active communities while homogeneous selection influenced the whole community assembly.

545   Our results combined with these previous studies indicate that community assembly of putatively-active

546   members may be more closely linked to short-term environmental change than assembly of the whole

547   community.

548

549   In addition to being more sensitive to disturbance, we find that assembly of the putatively active

550   community was more strongly tied to microbial processes (i.e., respiration rate), than was the whole

551   community. A strong link between biogeochemical rates and the putatively active community is

552   consistent with previous studies (Freedman et al., 2015; Levy-Booth et al., 2019). More specifically, we

553   observed a negative relationship between respiration rate and absolute values of βNTI for the putatively

554   active community, but no relationship for the whole community. The direction of this relationship is

555   opposite to our hypothesis. While stronger selection should remove mal-adapted individuals, leading to

556   higher biogeochemical rates (Graham and Stegen, 2017), increased selection in our experiment was

557   imposed by disturbance that appeared to directly suppress respiration rates due to desiccation (Baldwin

558   and Mitchell, 2000; Manzoni et al., 2012). The simultaneous suppression of respiration and imposition

559   of stronger selection in treatments with 31 or 34 days of dry conditions (Fig. 3b) led to the negative

560   relationship between respiration and the strength of selection. The lack of such relationships when

561   considering the whole community indicates that a greater focus on assembly dynamics of putatively

562   active communities could reveal new insights into the multi-component linkages among microbes, the

563   environment, and function.

564

565   Disturbance also impacted OM thermodynamics and respiration rates, potentially initiating an iterative

566   loop among microbial assembly, microbial processes, and the abiotic environment. In this iterative loop

567   the direction of causation between OM thermodynamics and microbial processes (Fig. 1, arrow 3) is not

568   clear due to feedbacks, though we interpret a direction of causation from OM thermodynamics to

569   microbial properties in terms of community assembly (Fig. 1 arrow 4). As such, there may be a loop

570   between OM thermodynamics and microbial processes (i.e., respiration) embedded in a larger loop that

571   also includes microbial properties (i.e., community assembly). Such feedbacks are inherent in complex

572   systems and often lead to non-linear dynamics as observed here in terms of the threshold-like impact of

573   desiccation on multiple system components (Pérez Castro et al., 2019; Prosser and Martiny, 2020).

574

575   As key elements of the inferred system of feedbacks, the links among OM thermodynamic properties,

576   respiration, and desiccation found here are consistent with recent work tied to the same field system.

577   That is, Garayburu-Caruso et al. (Garayburu-Caruso et al., 2020) also showed decreasing aerobic

578   respiration with decreasing favorability for oxidation (i.e., larger values of ΔG^0_{Cox}) using sediments

579   sourced ~2 years previously from the same field system. In addition, the impacts of desiccation found

580   here are similar to Goldman et al. (Goldman et al., 2017) after re-inundation. This impact of desiccation

581   on respiration contrasts with the Birch effect (Birch and Friend, 1956) in soils whereby desiccation

582   followed by re-wetting leads to enhanced respiration. The consistency across hyporheic zone studies and

583   deviation from classical soil phenomena points to potential consistency in governing processes within

584   the hyporheic zone that deviate from processes operating in soil systems. Further evaluation is needed

585   across additional hyporheic zone systems to rigorously evaluate this inference, however.

586

587 In addition to linkages between the environment and microbial aspects of the system, our study revealed

588 connections within the environmental components of the conceptual framework. That is, greater

589 cumulative desiccation caused an increase in ΔG^0_{Cox}, indicating a significant change in OM

590 thermodynamics (Fig. 5c). While our data cannot pinpoint governing mechanism(s), we hypothesize that

591 the ΔG^0_{Cox} response may have been tied to increased ion concentration following desiccation. For

592 example, OM chemistry may have been altered due to changes in abiotic sorption, limitations of

593 microbially accessible C due to water potential constraints, and/or osmolyte production and formation of

594 extracellular polymeric substances (Fierer et al., 2003; Gionchetta et al., 2020; Homyak et al., 2018).

595

596 Irrespective of mechanisms, the shift in OM thermodynamics in response to desiccation was associated

597 with a decline in respiration. We infer a causal connection between OM thermodynamics and

598 respiration, potentially triggered by desiccation-driven shifts in OM chemistry and/or microbial

599 physiology. This causal connection is supported by recent work (Garayburu-Caruso et al., 2020) and the

600 observation of a continuous function between ΔG^0_{Cox} and respiration rate that transcended experimental

601 treatments. Desiccation therefore likely influences and may even initiate an iterative loop among OM

602 thermodynamics, microbial assembly, and biogeochemistry that underlies cumulative system function.

603

604 Cumulative system function can often be driven by ecosystem control points (Bernhardt et al., 2017),

605 but we observed relatively little indication of such behavior. That is, estimates of control point influence

606 (CPI) were relatively low across most treatments. CPI is theoretically constrained to range from 0.5-1,

607 with lower values indicating smaller influences of control points. In our study, all but one treatment had

608 CPI between ~0.5 and 0.7. The associated distributions of respiration rates did not contain obvious

609 outliers such that we interpret CPI values in the 0.5-0.7 range to be relatively low and not strongly

610   influenced by control points or biogeochemical hot spots/moments (McClain et al., 2003). The treatment

611   with 31 cumulative days of desiccation diverged from the rest in having a CPI value of ~0.9. This large

612   CPI was due to a single outlier (Fig. 5a) such that most of the cumulative respiration across reactors was

613   contributed by that single reactor. We interpret that single reactor as a biogeochemical hot spot or

614   control point within that experimental treatment. It is unclear, however, what led to such behavior as

615   disturbance did not have any systematic influence on CPI.

616

617   A strength of CPI as a metric is that it allows for direct quantitative comparisons across studies, systems,

618   and scales. Ours is the first study to estimate CPI, however, such that we cannot yet make comparisons

619   to previous work. Through future comparisons it will be possible to evaluate the strengths, weaknesses,

620   and behavior of CPI. We expect that some patterns may emerge such as CPI having a greater likelihood

621   to reach very high values (near 1) in systems with relatively low rates on average. In these conditions,

622   even a modest quantitative increase in biogeochemical rates can lead to a large proportional change such

623   that most cumulative function is from a single point in space and/or time, resulting in large CPI. We also

624   expect that some biogeochemical processes will show greater variation in CPI than others, potentially

625   due to variation in degree of functional redundancy (Louca et al., 2018). For example, processes such as

626   respiration can be performed by numerous microbial taxa (i.e., there is high functional redundancy),

627   while others are more constrained to a relatively small number of taxa (e.g., ammonia oxidation). We

628   hypothesize that CPI may be lower on average and less variable across systems and scales for

629   biogeochemical processes with greater functional redundancy. Additional work will be needed to test

630   this hypothesis.

631

5 Conclusions

In this study we coupled intrinsic characteristics of natural hyporheic zone sediments with imposed constraints in the form of desiccation to evaluate an *a priori* conceptual framework modified from Hall et al. (Hall et al., 2018). Our results demonstrated strong and often non-linear connections among desiccation, OM thermodynamics, assembly of the putatively active microbial community, and respiration rates. Collating our results points to further modification of the framework into an *a posteriori* conceptual model containing nested feedback loops (**Fig. 6**). This conceptual model is consistent with the recently proposed unification of microbial ecology around the concepts of external forcing, internal dynamics, and historical contingencies (Stegen et al., 2018a). That is, we hypothesize that external forcing imposed by desiccation initiates multiple internal loops that drive biological and chemical dynamics that, in turn, underlie respiration responses to re-wetting that are contingent on desiccation history. The development of conceptual models such as this is key to incorporating additional mechanistic detail into predictive simulation models (e.g., reactive transport codes). We encourage further evaluation and improvement of both our *a priori* and *a posteriori* concepts across environmentally divergent conditions to generate knowledge that is transferable across systems.

Code availability

The R scripts used in this study are hosted on ESS-DIVE and will be provided to readers when requested. Null modeling scripts were based on those available at https://github.com/stegen/Stegen_etal_ISME_2013.

Data availability

652   Data are available on the ESS-DIVE archive at the following link (a data package will be

653   published prior to the manuscript being published, and the associated link will be provided).

654   Sequence data is available on NCBI's Sequence Read Archive PRJNA641165.

655   **Supplement**

656   The supplement related to this article is available online at: XXX

657   **Author contributions**

658   JCS and SF conceptualized and designed the study; JT, JW, LR, RC, SF, and VAG-C performed

659   the experiment; AS, JCS, RED, and SF analyzed data; AS, JCS, and SF drafted the manuscript

660   and all authors contributed to further writing.

661   **Competing interests**

662   The authors declare that they have no conflict of interest.

663   **Acknowledgements**

664   We thank Amy Goldman and Nathan Johnson for developing graphics. The initial experimental stages

665   of this work were supported by the PREMIS Initiative at the Pacific Northwest National Laboratory

666   (PNNL) with funding from the Laboratory Directed Research and Development Program at PNNL, a

667   multi-program national laboratory operated by Battelle for the US Department of Energy under Contract

668   DE-AC05-76RL01830. The later stages of this work (e.g., data analysis, conceptual interpretation,

669   manuscript development) were supported by the U.S. Department of Energy-BER program, as part of an

670   Early Career Award to JCS at PNNL. A portion of the research was performed using EMSL, a DOE

671   Office of Science User Facility sponsored by the Office of Biological and Environmental Research.

672

References

674 Arntzen, E.: Effects of fluctuating river flow on groundwater/surface water mixing in the hyporheic zone
675 of a regulated, large cobble bed river - Arntzen - 2006 - River Research and Applications - Wiley Online
676 Library, https://onlinelibrary.wiley.com/doi/abs/10.1002/rra.947, last access: 8 July 2020, 2006.
677
678 Arora, B., Briggs, M. A., Zarnetske, J., Stegen, J. C., Gomez-Velez, J., Dwivedi, D. and Steefel, C. I.:
679 Hot Spots and Hot Moments in the Critical Zone: Identification of and Incorporation into Reactive
680 Transport Models, in Biogeochemistry of the Critical Zone, edited by A. Wymore, W. Yang, W. Silver,
681 B. McDowell, and J. Chorover, Springer-Nature, , 2020.
682
683 Baldwin, D. S. and Mitchell, A. M.: The effects of drying and re-flooding on the sediment and soil
684 nutrient dynamics of lowland river–floodplain systems: a synthesis, Regul. Rivers Res. Manag., 16(5),
685 457–467, https://doi.org/10.1002/1099-1646(200009/10)16:5<457::AID-RRR597>3.0.CO;2-B, 2000.
686
687 Barnard, R. L., Osborne, C. A. and Firestone, M. K.: Changing precipitation pattern alters soil microbial
688 community response to wet-up under a Mediterranean-type climate, ISME J., 9(4), 946–957,
689 https://doi.org/10.1038/ismej.2014.192, 2015.
690
691 Bartelme, R. P., Custer, J. M., Dupont, C. L., Espinoza, J. L., Torralba, M., Khalili, B. and Carini, P.:
692 Influence of Substrate Concentration on the Culturability of Heterotrophic Soil Microbes Isolated by
693 High-Throughput Dilution-to-Extinction Cultivation, mSphere, 5(1),
694 https://doi.org/10.1128/mSphere.00024-20, 2020.
695
696 Behrens, S., Kappler, A. and Obst, M.: Linking environmental processes to the in situ functioning of
697 microorganisms by high-resolution secondary ion mass spectrometry (NanoSIMS) and scanning
698 transmission X-ray microscopy (STXM), Environ. Microbiol., 14(11), 2851–2869,
699 https://doi.org/10.1111/j.1462-2920.2012.02724.x, 2012.
700
701 Bernhardt, E. S., Blaszczak, J. R., Ficken, C. D., Fork, M. L., Kaiser, K. E. and Seybold, E. C.: Control
702 Points in Ecosystems: Moving Beyond the Hot Spot Hot Moment Concept, Ecosystems, 20(4), 665–682,
703 https://doi.org/10.1007/s10021-016-0103-y, 2017.
704
705 Bier, R. L., Bernhardt, E. S., Boot, C. M., Graham, E. B., Hall, E. K., Lennon, J. T., Nemergut, D. R.,
706 Osborne, B. B., Ruiz-González, C., Schimel, J. P., Waldrop, M. P. and Wallenstein, M. D.: Linking
707 microbial community structure and microbial processes: an empirical and conceptual overview, FEMS
708 Microbiol. Ecol., 91(10), https://doi.org/10.1093/femsec/fiv113, 2015.
709
710 Birch, H. F.: Mineralisation of plant nitrogen following alternate wet and dry conditions, Plant Soil,
711 20(1), 43–49, https://doi.org/10.1007/BF01378096, 1964.
712
713 Birch, H. F. and Friend, M. T.: Humus Decomposition in East African Soils, Nature, 178(4531), 500–
714 501, https://doi.org/10.1038/178500a0, 1956.
715
716 Blazewicz, S. J., Barnard, R. L., Daly, R. A. and Firestone, M. K.: Evaluating rRNA as an indicator of

microbial activity in environmental communities: limitations and uses, ISME J., 7(11), 2061–2068, https://doi.org/10.1038/ismej.2013.102, 2013.

Boano, F., Harvey, J. W., Marion, A., Packman, A. I., Revelli, R., Ridolfi, L. and Wörman, A.: Hyporheic flow and transport processes: Mechanisms, models, and biogeochemical implications, Rev. Geophys., 52(4), 603–679, https://doi.org/10.1002/2012RG000417, 2014.

Bottos, E. M., Kennedy, D. W., Romero, E. B., Fansler, S. J., Brown, J. M., Bramer, L. M., Chu, R. K., Tfaily, M. M., Jansson, J. K. and Stegen, J. C.: Dispersal limitation and thermodynamic constraints govern spatial structure of permafrost microbial communities, FEMS Microbiol. Ecol., 94(8), https://doi.org/10.1093/femsec/fiy110, 2018.

Boyd, E. S., Cummings, D. E. and Geesey, G. G.: Mineralogy Influences Structure and Diversity of Bacterial Communities Associated with Geological Substrata in a Pristine Aquifer, Microb. Ecol., 54(1), 170–182, https://doi.org/10.1007/s00248-006-9187-9, 2007.

Boye, K., Noël, V., Tfaily, M. M., Bone, S. E., Williams, K. H., Bargar, J. R. and Fendorf, S.: Thermodynamically controlled preservation of organic carbon in floodplains, Nat. Geosci., 10(6), 415–419, https://doi.org/10.1038/ngeo2940, 2017.

Brown, J., Zavoshy, N., Brislawn, C. J. and McCue, L. A.: Hundo: a Snakemake workflow for microbial community sequence data, PeerJ Inc., 2018.

Burrows, R. M., Rutlidge, H., Bond, N. R., Eberhard, S. M., Auhl, A., Andersen, M. S., Valdez, D. G. and Kennard, M. J.: High rates of organic carbon processing in the hyporheic zone of intermittent streams, Sci. Rep., 7(1), 1–11, https://doi.org/10.1038/s41598-017-12957-5, 2017.

Caporaso, J. G.: EMP 16S Illumina Amplicon Protocol, , https://doi.org/10.17504/protocols.io.nuudeww, 2018.

Cardoso, D. C., Sandionigi, A., Cretoiu, M. S., Casiraghi, M., Stal, L. and Bolhuis, H.: Comparison of the active and resident community of a coastal microbial mat, Sci. Rep., 7(1), 1–10, https://doi.org/10.1038/s41598-017-03095-z, 2017.

Carson, J. K., Campbell, L., Rooney, D., Clipson, N. and Gleeson, D. B.: Minerals in soil select distinct bacterial communities in their microhabitats, FEMS Microbiol. Ecol., 67(3), 381–388, https://doi.org/10.1111/j.1574-6941.2008.00645.x, 2009.

Chase, J. M.: Drought mediates the importance of stochastic community assembly, PNAS, 104, 17430–17434, https://doi.org/10.1073/pnas.0704350104, 2007.

Chen, W., Ren, K., Isabwe, A., Chen, H., Liu, M. and Yang, J.: Stochastic processes shape microeukaryotic community assembly in a subtropical river across wet and dry seasons, Microbiome, 7(1), 138, https://doi.org/10.1186/s40168-019-0749-8, 2019.

Daly, R. A., Borton, M. A., Wilkins, M. J., Hoyt, D. W., Kountz, D. J., Wolfe, R. A., Welch, S. A.,

763   Marcus, D. N., Trexler, R. V., MacRae, J. D., Krzycki, J. A., Cole, D. R., Mouser, P. J. and Wrighton,
764   K. C.: Microbial metabolisms in a 2.5-km-deep ecosystem created by hydraulic fracturing in shales, Nat.
765   Microbiol., 1(10), 1–9, https://doi.org/10.1038/nmicrobiol.2016.146, 2016.
766

767   Danczak, R. E., Goldman, A. E., Chu, R. K., Toyoda, J. G., Garayburu-Caruso, V. A., Tolić, N.,
768   Graham, E. B., Morad, J. W., Renteria, L., Wells, J. R., Herzog, S. P., Ward, A. S. and Stegen, J. C.:
769   Ecological theory applied to environmental metabolomes reveals compositional divergence despite
770   conserved molecular properties, bioRxiv, 2020.02.12.946459,
771   https://doi.org/10.1101/2020.02.12.946459, 2020.
772

773   Demars, B. O. L.: Hydrological pulses and burning of dissolved organic carbon by stream respiration,
774   Limnol. Oceanogr., 64(1), 406–421, https://doi.org/10.1002/lno.11048, 2019.
775

776   Dini-Andreote, F., Stegen, J. C., Elsas, J. D. van and Salles, J. F.: Disentangling mechanisms that
777   mediate the balance between stochastic and deterministic processes in microbial succession, Proc. Natl.
778   Acad. Sci., 112(11), E1326–E1332, https://doi.org/10.1073/pnas.1414261112, 2015.
779

780   Doetterl, S., Berhe, A. A., Arnold, C., Bodé, S., Fiener, P., Finke, P., Fuchslueger, L., Griepentrog, M.,
781   Harden, J. W., Nadeu, E., Schnecker, J., Six, J., Trumbore, S., Van Oost, K., Vogel, C. and Boeckx, P.:
782   Links among warming, carbon and microbial dynamics mediated by soil mineral weathering, Nat.
783   Geosci., 11(8), 589–593, https://doi.org/10.1038/s41561-018-0168-7, 2018.
784

785   Fatichi, S., Manzoni, S., Or, D. and Paschalis, A.: A Mechanistic Model of Microbially Mediated Soil
786   Biogeochemical Processes: A Reality Check, Glob. Biogeochem. Cycles, 33(6), 620–648,
787   https://doi.org/10.1029/2018GB006077, 2019.
788

789   Fauvel, B., Cauchie, H.-M., Gantzer, C. and Ogorzaly, L.: Influence of physico-chemical characteristics
790   of sediment on the in situ spatial distribution of F-specific RNA phages in the riverbed, FEMS
791   Microbiol. Ecol., 95(2), https://doi.org/10.1093/femsec/fiy240, 2019.
792

793   Feng, Y., Chen, R., Stegen, J. C., Guo, Z., Zhang, J., Li, Z. and Lin, X.: Two key features influencing
794   community assembly processes at regional scale: Initial state and degree of change in environmental
795   conditions, Mol. Ecol., 27(24), 5238–5251, https://doi.org/10.1111/mec.14914, 2018.
796

797   Fierer, N., Allen, A. S., Schimel, J. P. and Holden, P. A.: Controls on microbial CO2 production: a
798   comparison of surface and subsurface soil horizons, Glob. Change Biol., 9(9), 1322–1332,
799   https://doi.org/10.1046/j.1365-2486.2003.00663.x, 2003.
800

801   Fillinger, L., Zhou, Y., Kellermann, C. and Griebler, C.: Non-random processes determine the
802   colonization of groundwater sediments by microbial communities in a pristine porous aquifer, Environ.
803   Microbiol., 21(1), 327–342, https://doi.org/10.1111/1462-2920.14463, 2019.
804

805   Fischer, H., Kloep, F., Wilzcek, S. and Pusch, M. T.: A River's Liver – Microbial Processes within the
806   Hyporheic Zone of a Large Lowland River, Biogeochemistry, 76(2), 349–371,
807   https://doi.org/10.1007/s10533-005-6896-y, 2005.
808

809 Freedman, Z. B., Romanowicz, K. J., Upchurch, R. A. and Zak, D. R.: Differential responses of total
810 and active soil microbial communities to long-term experimental N deposition, Soil Biol. Biochem., 90,
811 275–282, https://doi.org/10.1016/j.soilbio.2015.08.014, 2015.

813 Fu, X., Li, Y., Meng, Y., Yuan, Q., Zhang, Z., Norbäck, D., Deng, Y., Zhang, X. and Sun, Y.: Derived
814 ecological niches of indoor microbes are crucial for asthma symptoms in university dormitories,
815 bioRxiv, 2020.01.05.893529, https://doi.org/10.1101/2020.01.05.893529, 2020.

817 Garayburu-Caruso, V. A., Stegen, J. C., Song, H.-S., Renteria, L., Wells, J., Garcia, W., Resch, C. T.,
818 Goldman, A. E., Chu, R. K., Toyoda, J. and Graham, E. B.: Carbon Limitation Leads to Thermodynamic
819 Regulation of Aerobic Metabolism, Environ. Sci. Technol. Lett.,
820 https://doi.org/10.1021/acs.estlett.0c00258, 2020.

822 Gilbert, J. A., Jansson, J. K. and Knight, R.: Earth Microbiome Project and Global Systems Biology,
823 mSystems, 3(3), https://doi.org/10.1128/mSystems.00217-17, 2018.

825 Gionchetta, G., Oliva, F., Romani, A. M. and Baneras, L.: Hydrological variations shape diversity and
826 functional responses of streambed microbes, Sci. Total Environ., 714, 136838,
827 https://doi.org/10.1016/j.scitotenv.2020.136838, 2020.

829 Goldman, A. E., Graham, E. B., Crump, A. R., Kennedy, D. W., Romero, E. B., Anderson, C. G., Dana,
830 K. L., Resch, C. T., Fredrickson, J. K. and Stegen, J. C.: Biogeochemical cycling at the aquatic–
831 terrestrial interface is linked to parafluvial hyporheic zone inundation history, Biogeosciences, 14(18),
832 4229–4241, https://doi.org/10.5194/bg-14-4229-2017, 2017.

834 Graham, E. B. and Stegen, J. C.: Dispersal-Based Microbial Community Assembly Decreases
835 Biogeochemical Function, Processes, 5(4), 65, https://doi.org/10.3390/pr5040065, 2017.

837 Graham, E. B., Crump, A. R., Resch, C. T., Fansler, S., Arntzen, E., Kennedy, D. W., Fredrickson, J. K.
838 and Stegen, J. C.: Coupling Spatiotemporal Community Assembly Processes to Changes in Microbial
839 Metabolism, Front. Microbiol., 7, https://doi.org/10.3389/fmicb.2016.01949, 2016.

841 Graham, E. B., Tfaily, M. M., Crump, A. R., Goldman, A. E., Bramer, L. M., Arntzen, E., Romero, E.,
842 Resch, C. T., Kennedy, D. W. and Stegen, J. C.: Carbon Inputs From Riparian Vegetation Limit
843 Oxidation of Physically Bound Organic Carbon Via Biochemical and Thermodynamic Processes, J.
844 Geophys. Res. Biogeosciences, 122(12), 3188–3205, https://doi.org/10.1002/2017JG003967, 2017a.

846 Graham, E. B., Crump, A. R., Resch, C. T., Fansler, S., Arntzen, E., Kennedy, D. W., Fredrickson, J. K.
847 and Stegen, J. C.: Deterministic influences exceed dispersal effects on hydrologically-connected
848 microbiomes, Environ. Microbiol., 19(4), 1552–1567, https://doi.org/10.1111/1462-2920.13720, 2017b.

850 Graham, E. B., Crump, A. R., Kennedy, D. W., Arntzen, E., Fansler, S., Purvine, S. O., Nicora, C. D.,
851 Nelson, W., Tfaily, M. M. and Stegen, J. C.: Multi 'omics comparison reveals metabolome
852 biochemistry, not microbiome composition or gene expression, corresponds to elevated biogeochemical
853 function in the hyporheic zone, Sci. Total Environ., 642, 742–753,
854 https://doi.org/10.1016/j.scitotenv.2018.05.256, 2018.

855

856 Grilli, J., Barabás, G., Michalska-Smith, M. J. and Allesina, S.: Higher-order interactions stabilize
857 dynamics in competitive network models, Nature, 548(7666), 210–213,
858 https://doi.org/10.1038/nature23273, 2017.

859

860 Hall, E. K., Bernhardt, E. S., Bier, R. L., Bradford, M. A., Boot, C. M., Cotner, J. B., del Giorgio, P. A.,
861 Evans, S. E., Graham, E. B., Jones, S. E., Lennon, J. T., Locey, K. J., Nemergut, D., Osborne, B. B.,
862 Rocca, J. D., Schimel, J. P., Waldrop, M. P. and Wallenstein, M. D.: Understanding how microbiomes
863 influence the systems they inhabit, Nat. Microbiol., 3(9), 977–982, https://doi.org/10.1038/s41564-018-
864 0201-z, 2018.

865

866 Homyak, P. M., Blankinship, J. C., Slessarev, E. W., Schaeffer, S. M., Manzoni, S. and Schimel, J. P.:
867 Effects of altered dry season length and plant inputs on soluble soil carbon, Ecology, 99(10), 2348–
868 2362, https://doi.org/10.1002/ecy.2473, 2018.

869

870 Jia, X., Dini-Andreote, F. and Falcão Salles, J.: Comparing the Influence of Assembly Processes
871 Governing Bacterial Community Succession Based on DNA and RNA Data, Microorganisms, 8(6), 798,
872 https://doi.org/10.3390/microorganisms8060798, 2020.

873

874 Jurburg, S. D., Nunes, I., Stegen, J. C., Le Roux, X., Priemé, A., Sørensen, S. J. and Salles, J. F.:
875 Autogenic succession and deterministic recovery following disturbance in soil bacterial communities,
876 Sci. Rep., 7(1), 1–11, https://doi.org/10.1038/srep45691, 2017.

877

878 Kaufman, M. H., Cardenas, M. B., Buttles, J., Kessler, A. J. and Cook, P. L. M.: Hyporheic hot
879 moments: Dissolved oxygen dynamics in the hyporheic zone in response to surface flow perturbations,
880 Water Resour. Res., 53(8), 6642–6662, https://doi.org/10.1002/2016WR020296, 2017.

881

882 Kearns, P. J., Angell, J. H., Howard, E. M., Deegan, L. A., Stanley, R. H. R. and Bowen, J. L.: Nutrient
883 enrichment induces dormancy and decreases diversity of active bacteria in salt marsh sediments, Nat.
884 Commun., 7(1), 12881, https://doi.org/10.1038/ncomms12881, 2016.

885

886 König, S., Worrich, A., Banitz, T., Centler, F., Harms, H., Kästner, M., Miltner, A., Wick, L. Y.,
887 Thullner, M. and Frank, K.: Spatiotemporal disturbance characteristics determine functional stability
888 and collapse risk of simulated microbial ecosystems, Sci. Rep., 8(1), 1–13,
889 https://doi.org/10.1038/s41598-018-27785-4, 2018.

890

891 Larned, S. T., Datry, T., Arscott, D. B. and Tockner, K.: Emerging concepts in temporary-river ecology,
892 Freshw. Biol., 55(4), 717–738, https://doi.org/10.1111/j.1365-2427.2009.02322.x, 2010.

893

894 LaRowe, D. E. and Van Cappellen, P.: Degradation of natural organic matter: A thermodynamic
895 analysis, Geochim. Cosmochim. Acta, 75(8), 2030–2042, https://doi.org/10.1016/j.gca.2011.01.020,
896 2011.

897

898 Leventhal, G. E., Ackermann, M. and Schiessl, K. T.: Why microbes secrete molecules to modify their
899 environment: the case of iron-chelating siderophores, J. R. Soc. Interface, 16(150), 20180674,
900 https://doi.org/10.1098/rsif.2018.0674, 2019.

901

902 Levy-Booth, D. J., Giesbrecht, I. J. W., Kellogg, C. T. E., Heger, T. J., D'Amore, D. V., Keeling, P. J.,
903 Hallam, S. J. and Mohn, W. W.: Seasonal and ecohydrological regulation of active microbial
904 populations involved in DOC, CO 2 , and CH 4 fluxes in temperate rainforest soil, ISME J., 13(4), 950–
905 963, https://doi.org/10.1038/s41396-018-0334-3, 2019.

906

907 Li, Y., Gao, Y., Zhang, W., Wang, C., Wang, P., Niu, L. and Wu, H.: Homogeneous selection dominates
908 the microbial community assembly in the sediment of the Three Gorges Reservoir, Sci. Total Environ.,
909 690, 50–60, https://doi.org/10.1016/j.scitotenv.2019.07.014, 2019.

910

911 Lloyd-Price, J., Arze, C., Ananthakrishnan, A. N., Schirmer, M., Avila-Pacheco, J., Poon, T. W.,
912 Andrews, E., Ajami, N. J., Bonham, K. S., Brislawn, C. J., Casero, D., Courtney, H., Gonzalez, A.,
913 Graeber, T. G., Hall, A. B., Lake, K., Landers, C. J., Mallick, H., Plichta, D. R., Prasad, M., Rahnavard,
914 G., Sauk, J., Shungin, D., Vázquez-Baeza, Y., White, R. A., Braun, J., Denson, L. A., Jansson, J. K.,
915 Knight, R., Kugathasan, S., McGovern, D. P. B., Petrosino, J. F., Stappenbeck, T. S., Winter, H. S.,
916 Clish, C. B., Franzosa, E. A., Vlamakis, H., Xavier, R. J. and Huttenhower, C.: Multi-omics of the gut
917 microbial ecosystem in inflammatory bowel diseases, Nature, 569(7758), 655–662,
918 https://doi.org/10.1038/s41586-019-1237-9, 2019.

919

920 Louca, S., Polz, M. F., Mazel, F., Albright, M. B. N., Huber, J. A., O'Connor, M. I., Ackermann, M.,
921 Hahn, A. S., Srivastava, D. S., Crowe, S. A., Doebeli, M. and Parfrey, L. W.: Function and functional
922 redundancy in microbial systems, Nat. Ecol. Evol., 2(6), 936–943, https://doi.org/10.1038/s41559-018-
923 0519-1, 2018.

924

925 Malik, A. A., Martiny, J. B. H., Brodie, E. L., Martiny, A. C., Treseder, K. K. and Allison, S. D.:
926 Defining trait-based microbial strategies with consequences for soil carbon cycling under climate
927 change, ISME J., 14(1), 1–9, https://doi.org/10.1038/s41396-019-0510-0, 2020.

928

929 Manzella, M., Geiss, R. and Hall, E. K.: Evaluating the stoichiometric trait distributions of cultured
930 bacterial populations and uncultured microbial communities, Environ. Microbiol., 21(10), 3613–3626,
931 https://doi.org/10.1111/1462-2920.14684, 2019.

932

933 Manzoni, S., Schimel, J. P. and Porporato, A.: Responses of soil microbial communities to water stress:
934 results from a meta-analysis, Ecology, 93(4), 930–938, https://doi.org/10.1890/11-0026.1, 2012.

935

936 Martínez, I., Stegen, J. C., Maldonado-Gómez, M. X., Eren, A. M., Siba, P. M., Greenhill, A. R. and
937 Walter, J.: The Gut Microbiota of Rural Papua New Guineans: Composition, Diversity Patterns, and
938 Ecological Processes, Cell Rep., 11(4), 527–538, https://doi.org/10.1016/j.celrep.2015.03.049, 2015.
939 Mauck, B. S. and Roberts, J. A.: Mineralogic Control on Abundance and Diversity of Surface-Adherent
940 Microbial Communities, Geomicrobiol. J., 24(3–4), 167–177,
941 https://doi.org/10.1080/01490450701457162, 2007.

942

943 McClain, M. E., Boyer, E. W., Dent, C. L., Gergel, S. E., Grimm, N. B., Groffman, P. M., Hart, S. C.,
944 Harvey, J. W., Johnston, C. A., Mayorga, E., McDowell, W. H. and Pinay, G.: Biogeochemical Hot
945 Spots and Hot Moments at the Interface of Terrestrial and Aquatic Ecosystems, Ecosystems, 6(4), 301–
946 312, https://doi.org/10.1007/s10021-003-0161-9, 2003.

947

948 Norland, S., Fagerbakke, K. M. and Heldal, M.: Light element analysis of individual bacteria by x-ray
949 microanalysis., Appl. Environ. Microbiol., 61(4), 1357–1362, https://doi.org/10.1128/AEM.61.4.1357-
950 1362.1995, 1995.

951

952 Ofiţeru, I. D., Lunn, M., Curtis, T. P., Wells, G. F., Criddle, C. S., Francis, C. A. and Sloan, W. T.:
953 Combined niche and neutral effects in a microbial wastewater treatment community, Proc. Natl. Acad.
954 Sci., 107(35), 15345–15350, https://doi.org/10.1073/pnas.1000604107, 2010.

955

956 Pérez Castro, S., Cleland, E. E., Wagner, R., Sawad, R. A. and Lipson, D. A.: Soil microbial responses
957 to drought and exotic plants shift carbon metabolism, ISME J., 13(7), 1776–1787,
958 https://doi.org/10.1038/s41396-019-0389-9, 2019.

959

960 Prosser, J. I. and Martiny, J. B. H.: Conceptual challenges in microbial community ecology, Philos.
961 Trans. R. Soc. B Biol. Sci., 375(1798), 20190241, https://doi.org/10.1098/rstb.2019.0241, 2020.
962 Ratzke, C., Denk, J. and Gore, J.: Ecological suicide in microbes, Nat. Ecol. Evol., 2(5), 867–872,
963 https://doi.org/10.1038/s41559-018-0535-1, 2018.

964

965 Romaní, A. M., Vázquez, E. and Butturini, A.: Microbial Availability and Size Fractionation of
966 Dissolved Organic Carbon After Drought in an Intermittent Stream: Biogeochemical Link Across the
967 Stream–Riparian Interface, Microb. Ecol., 52(3), 501–512, https://doi.org/10.1007/s00248-006-9112-2,
968 2006.

969

970 Sengupta, A., Stegen, J. C., Neto, A. A. M., Wang, Y., Neilson, J. W., Tatarin, T., Hunt, E., Dontsova,
971 K., Chorover, J., Troch, P. A. and Maier, R. M.: Assessing Microbial Community Patterns During
972 Incipient Soil Formation From Basalt, J. Geophys. Res. Biogeosciences, 124(4), 941–958,
973 https://doi.org/10.1029/2017JG004315, 2019a.

974

975 Sengupta, A., Indivero, J., Gunn, C., Tfaily, M. M., Chu, R. K., Toyoda, J., Bailey, V. L., Ward, N. D.
976 and Stegen, J. C.: Spatial gradients in the characteristics of soil-carbon fractions are associated with
977 abiotic features but not microbial communities, Biogeosciences, 16(19), 3911–3928,
978 https://doi.org/10.5194/bg-16-3911-2019, 2019b.

979

980 Shu, D., Guo, J., Zhang, B., He, Y. and Wei, G.: rDNA- and rRNA-derived communities present
981 divergent assemblage patterns and functional traits throughout full-scale landfill leachate treatment
982 process trains, Sci. Total Environ., 646, 1069–1079, https://doi.org/10.1016/j.scitotenv.2018.07.388,
983 2019.

984

985 Slater, L. D., Ntarlagiannis, D., Day-Lewis, F. D., Mwakanyamale, K., Versteeg, R. J., Ward, A.,
986 Strickland, C., Johnson, C. D. and Lane, J. W.: Use of electrical imaging and distributed temperature
987 sensing methods to characterize surface water–groundwater exchange regulating uranium transport at
988 the Hanford 300 Area, Washington, Water Resour. Res., 46(10),
989 https://doi.org/10.1029/2010WR009110, 2010.

990

991 Song, H.-S., Stegen, J. C., Graham, E. B., Lee, J.-Y., Garayburu-Caruso, V. A., Nelson, W. C., Chen,
992 X., Moulton, J. D. and Scheibe, T. D.: Representing Organic Matter Thermodynamics in

Biogeochemical Reactions via Substrate-Explicit Modeling, bioRxiv, 2020.02.27.968669, https://doi.org/10.1101/2020.02.27.968669, 2020.

Starnawski, P., Bataillon, T., Ettema, T. J. G., Jochum, L. M., Schreiber, L., Chen, X., Lever, M. A., Polz, M. F., Jørgensen, B. B., Schramm, A. and Kjeldsen, K. U.: Microbial community assembly and evolution in subseafloor sediment, Proc. Natl. Acad. Sci., 114(11), 2940–2945, https://doi.org/10.1073/pnas.1614190114, 2017.

Stegen, J. C., Lin, X., Konopka, A. E. and Fredrickson, J. K.: Stochastic and deterministic assembly processes in subsurface microbial communities, ISME J., 6(9), 1653–1664, https://doi.org/10.1038/ismej.2012.22, 2012.

Stegen, J. C., Lin, X., Fredrickson, J. K., Chen, X., Kennedy, D. W., Murray, C. J., Rockhold, M. L. and Konopka, A.: Quantifying community assembly processes and identifying features that impose them, ISME J., 7(11), 2069–2079, https://doi.org/10.1038/ismej.2013.93, 2013.

Stegen, J. C., Lin, X., Fredrickson, J. K. and Konopka, A. E.: Estimating and mapping ecological processes influencing microbial community assembly, Front. Microbiol., 6, https://doi.org/10.3389/fmicb.2015.00370, 2015.

Stegen, J. C., Konopka, A., McKinley, J. P., Murray, C., Lin, X., Miller, M. D., Kennedy, D. W., Miller, E. A., Resch, C. T. and Fredrickson, J. K.: Coupling among Microbial Communities, Biogeochemistry and Mineralogy across Biogeochemical Facies, Sci. Rep., 6(1), 1–14, https://doi.org/10.1038/srep30553, 2016.

Stegen, J. C., Bottos, E. M. and Jansson, J. K.: A unified conceptual framework for prediction and control of microbiomes., Curr. Opin. Microbiol., https://doi.org/10.1016/j.mib.2018.06.002, 2018a.

Stegen, J. C., Johnson, T., Fredrickson, J. K., Wilkins, M. J., Konopka, A. E., Nelson, W. C., Arntzen, E. V., Chrisler, W. B., Chu, R. K., Fansler, S. J., Graham, E. B., Kennedy, D. W., Resch, C. T., Tfaily, M. and Zachara, J.: Influences of organic carbon speciation on hyporheic corridor biogeochemistry and microbial ecology, Nat. Commun., 9(1), 1–11, https://doi.org/10.1038/s41467-018-02922-9, 2018b.

Thompson, L. R., Sanders, J. G., McDonald, D., Amir, A., Ladau, J., Locey, K. J., Prill, R. J., Tripathi, A., Gibbons, S. M., Ackermann, G., Navas-Molina, J. A., Janssen, S., Kopylova, E., Vázquez-Baeza, Y., González, A., Morton, J. T., Mirarab, S., Zech Xu, Z., Jiang, L., Haroon, M. F., Kanbar, J., Zhu, Q., Jin Song, S., Kosciolek, T., Bokulich, N. A., Lefler, J., Brislawn, C. J., Humphrey, G., Owens, S. M., Hampton-Marcell, J., Berg-Lyons, D., McKenzie, V., Fierer, N., Fuhrman, J. A., Clauset, A., Stevens, R. L., Shade, A., Pollard, K. S., Goodwin, K. D., Jansson, J. K., Gilbert, J. A. and Knight, R.: A communal catalogue reveals Earth's multiscale microbial diversity, Nature, 551(7681), 457–463, https://doi.org/10.1038/nature24621, 2017.

Tripathi, B. M., Stegen, J. C., Kim, M., Dong, K., Adams, J. M. and Lee, Y. K.: Soil pH mediates the balance between stochastic and deterministic assembly of bacteria, ISME J., 12(4), 1072–1083, https://doi.org/10.1038/s41396-018-0082-4, 2018.

1039 Wagner, M.: Single-cell ecophysiology of microbes as revealed by Raman microspectroscopy or
1040 secondary ion mass spectrometry imaging, Annu. Rev. Microbiol., 63, 411–429,
1041 https://doi.org/10.1146/annurev.micro.091208.073233, 2009.
1042
1043 Wallenstein, M. D. and Hall, E. K.: A trait-based framework for predicting when and where microbial
1044 adaptation to climate change will affect ecosystem functioning, Biogeochemistry, 109(1), 35–47,
1045 https://doi.org/10.1007/s10533-011-9641-8, 2012.
1046
1047 Wang, J., Shen, J., Wu, Y., Tu, C., Soininen, J., Stegen, J. C., He, J., Liu, X., Zhang, L. and Zhang, E.:
1048 Phylogenetic beta diversity in bacterial assemblages across ecosystems: deterministic versus stochastic
1049 processes, ISME J., 7(7), 1310–1321, https://doi.org/10.1038/ismej.2013.30, 2013.
1050
1051 Whitman, T., Neurath, R., Perera, A., Chu-Jacoby, I., Ning, D., Zhou, J., Nico, P., Pett-Ridge, J. and
1052 Firestone, M.: Microbial community assembly differs across minerals in a rhizosphere microcosm,
1053 Environ. Microbiol., 20(12), 4444–4460, https://doi.org/10.1111/1462-2920.14366, 2018.
1054
1055 Wieder, W. R., Allison, S. D., Davidson, E. A., Georgiou, K., Hararuk, O., He, Y., Hopkins, F., Luo, Y.,
1056 Smith, M. J., Sulman, B., Todd-Brown, K., Wang, Y.-P., Xia, J. and Xu, X.: Explicitly representing soil
1057 microbial processes in Earth system models, Glob. Biogeochem. Cycles, 29(10), 1782–1800,
1058 https://doi.org/10.1002/2015GB005188, 2015.
1059
1060 Wisnoski, N. I., Muscarella, M. E., Larsen, M. L., Peralta, A. L. and Lennon, J. T.: Metabolic insight
1061 into bacterial community assembly across ecosystem boundaries, Ecology, 101(4), e02968,
1062 https://doi.org/10.1002/ecy.2968, 2020.
1063
1064 Wu, W., Lu, H.-P., Sastri, A., Yeh, Y.-C., Gong, G.-C., Chou, W.-C. and Hsieh, C.-H.: Contrasting the
1065 relative importance of species sorting and dispersal limitation in shaping marine bacterial versus protist
1066 communities, ISME J., 12(2), 485–494, https://doi.org/10.1038/ismej.2017.183, 2018.
1067
1068 Zachara, J. M., Long, P. E., Bargar, J., Davis, J. A., Fox, P., Fredrickson, J. K., Freshley, M. D.,
1069 Konopka, A. E., Liu, C., McKinley, J. P., Rockhold, M. L., Williams, K. H. and Yabusaki, S. B.:
1070 Persistence of uranium groundwater plumes: Contrasting mechanisms at two DOE sites in the
1071 groundwater–river interaction zone, J. Contam. Hydrol., 147, 45–72,
1072 https://doi.org/10.1016/j.jconhyd.2013.02.001, 2013.
1073
1074 Zhou, J. and Ning, D.: Stochastic Community Assembly: Does It Matter in Microbial Ecology?,
1075 Microbiol. Mol. Biol. Rev., 81(4), https://doi.org/10.1128/MMBR.00002-17, 2017.
1076
1077 Zhou, J., Liu, W., Deng, Y., Jiang, Y.-H., Xue, K., He, Z., Nostrand, J. D. V., Wu, L., Yang, Y. and
1078 Wang, A.: Stochastic Assembly Leads to Alternative Communities with Distinct Functions in a
1079 Bioreactor Microbial Community, mBio, 4(2), https://doi.org/10.1128/mBio.00584-12, 2013.
1080
1081
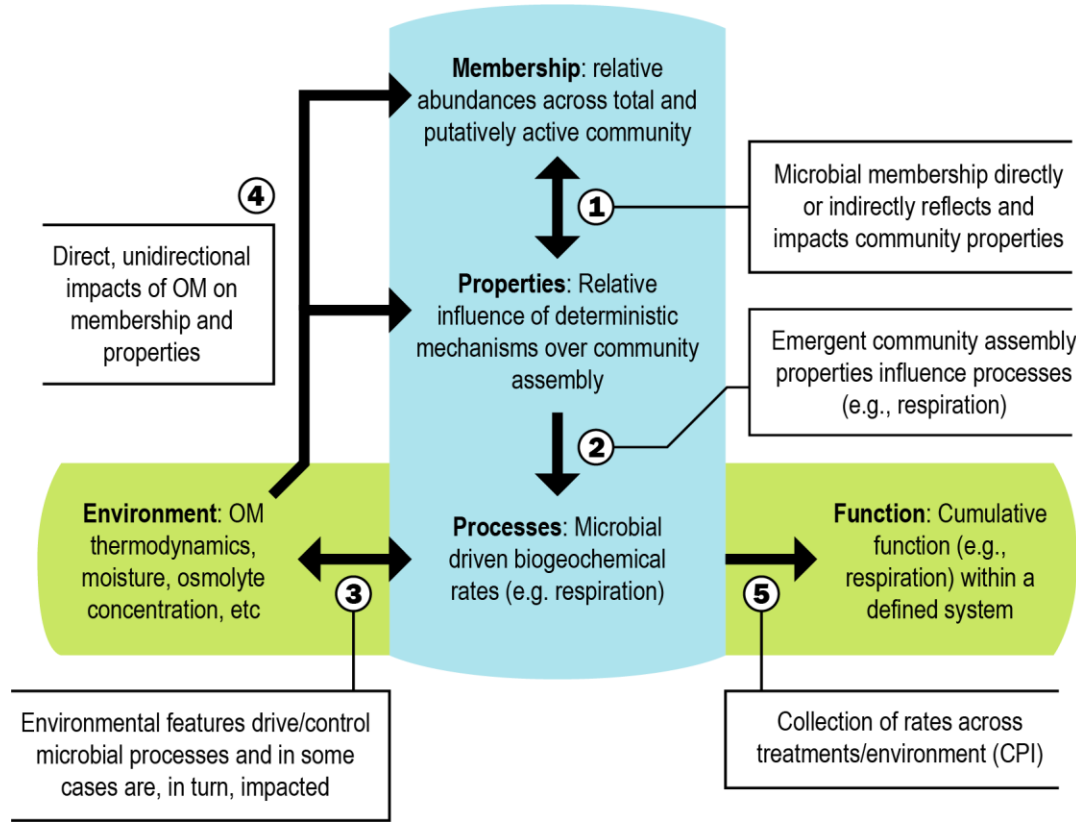
1084
1085
1086 **Figure 1. Integrated conceptual framework.** The conceptual figure (modified from Hall et al. (2018))
1087 details relationships (indicated by numbered arrows) between cumulative properties of the microbial
1088 community (*e.g.*, microbial membership, community assembly properties, biogeochemical rates),
1089 environmental features [*e.g.*, organic matter (OM) thermodynamics], and emergent ecosystem function
1090 [e.g., control point influence (CPI)]. Double headed arrows indicate feedbacks.
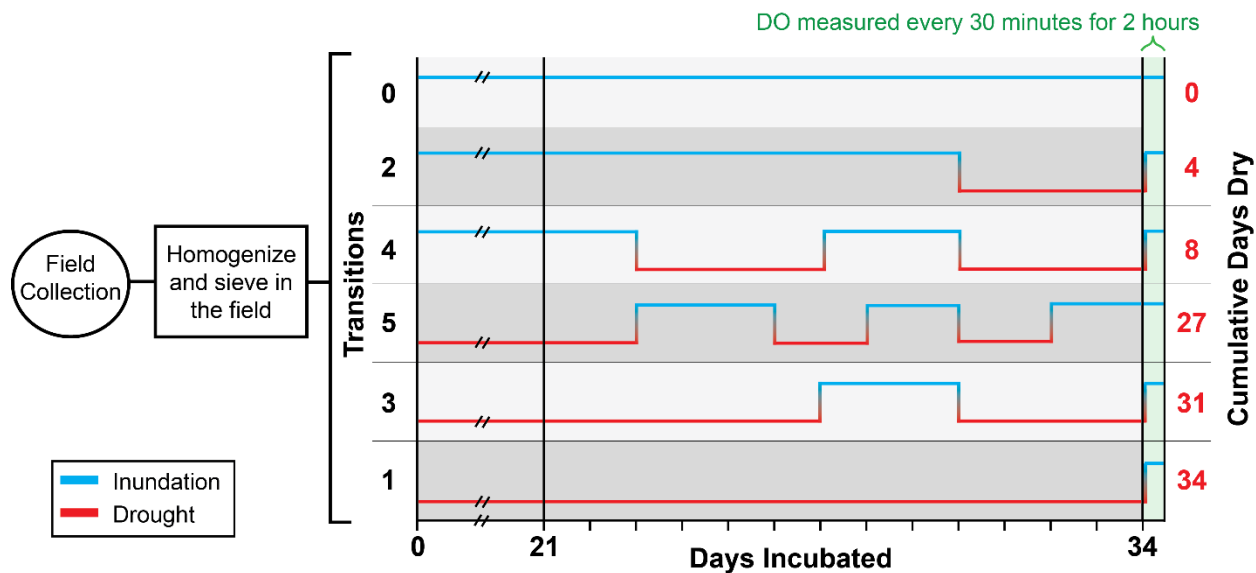
1091
1092
1093
1094 **Figure 2. Experimental design of batch reactor incubations subjected to six treatment regimes**
1095 **of inundated (blue line) and dry (red line) conditions.** Black values on the left indicate the number of
1096 inundated/dry transitions, including the final inundation that all treatments experienced immediately
1097 prior to the measurement of respiration. Red values on the right indicate the number of cumulative dry
1098 days (e.g., treatments with 1 or 3 transitions experienced 34 or 31 cumulative dry days, respectively.
1099 Transitions between inundated and dry conditions started on day 24. All treatments were held at either
1100 an inundated or dry state prior to day 24. Treatments are ordered by the number of days dry.
1101
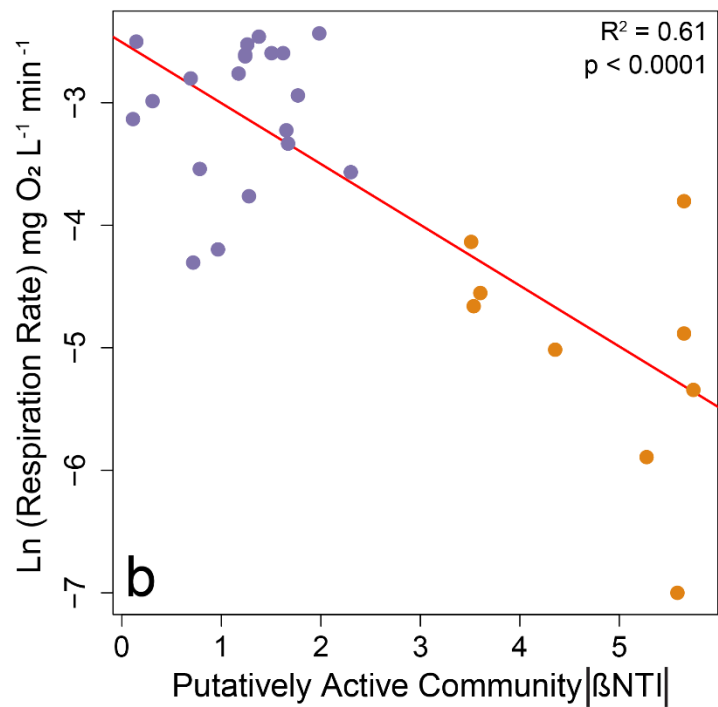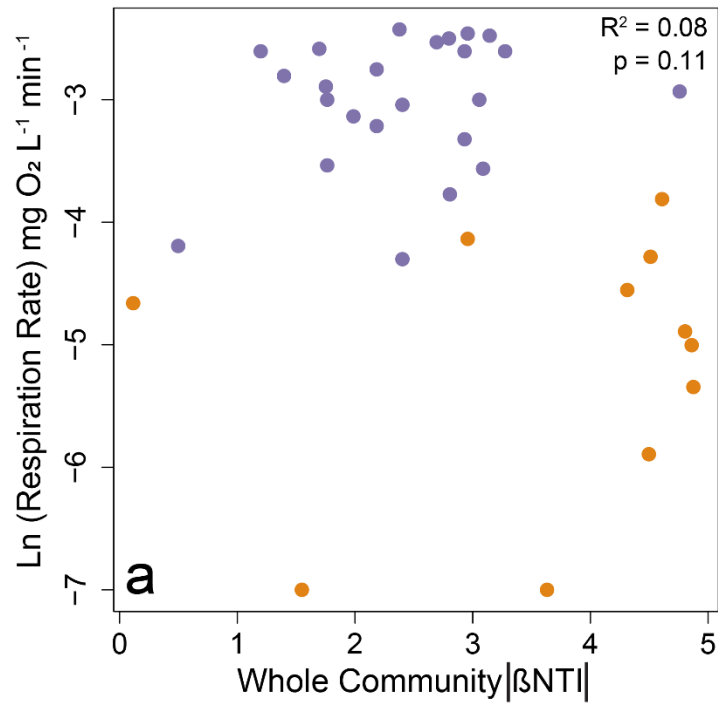
1102
1103
1104 **Figure 3. Natural log transformed respiration rates (i.e., O₂ consumption) as a function of the**
1105 **absolute value of βNTI for (a) whole communities or (b) putatively active communities.** Larger absolute
1106 values of βNTI indicate stronger influences of deterministic assembly. Nonlinearity was observed because the
1107 respiration rate has a lower limit of 0 such that its relationship with βNTI was fit as a negative exponential
1108 function. The significant regression model is shown as a red line, and statistics are provided on each panel.
1109 Treatments with 0, 4, 8, or 27 days dry are shown in purple. Treatments with 31or 34 days dry are shown in
1110 orange.
1111

1112
1113 **Figure 4. Boxplot representations of respiration rate (a) and putatively active community βNTI**
1114 **(b) distributions as a function of the cumulative number of days reactors were in a dried state.**
1115 Each value along the horizontal axis represents a different experimental treatment. On both panels the
1116 right hand axis provides estimates of control point influence (blue circles and lines) across the
1117 treatments. Horizontal red lines in (b) indicate significance thresholds; values below -2 indicate
1118 deterministic homogenous selection, values above +2 indicate deterministic variable selection, and
1119 values between -2 and +2 indicate stochastic assembly.
1120
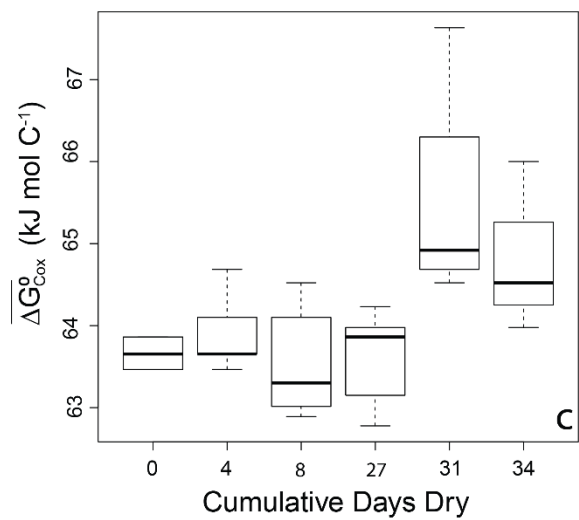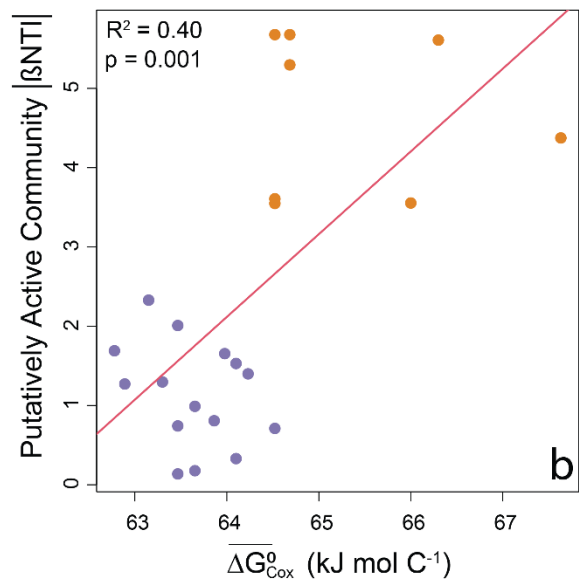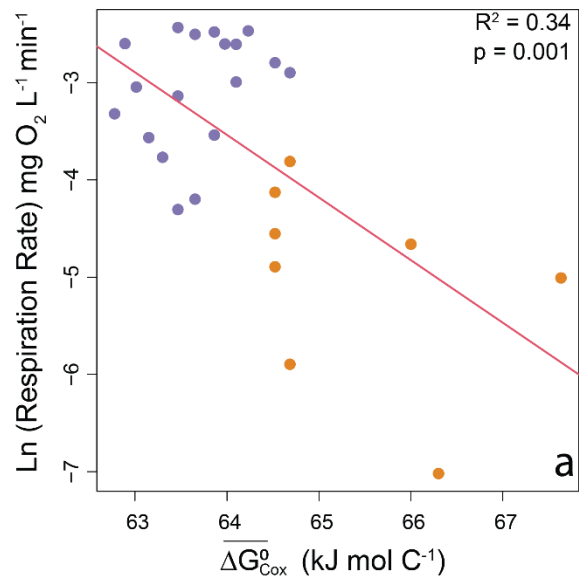
1122 **Figure 5. Microbial processes and properties as a function of OM thermodynamics, and impacts**
1123 **of disturbance on OM thermodynamics.** (a) Respiration rates (natural log transformed) decreased
1124 with decreasing favorability for oxidation (larger values of ΔG^0_{Cox}). (b) The strength of deterministic
1125 selection measured as the absolute value of βNTI increased with decreasing favorability for oxidation. Regression
1126 models are shown as red lines and statistics are provided on each panel. (c) Boxplot representations of the
1127 distributions of OM thermodynamics across experimental treatments. Significant increases were observed for
1128 treatments with 31 or 34 cumulative dry days. See text and Figure S7 for a description of statistics. Treatments
1129 with 0, 4, 8, or 27 days dry are shown in purple. Treatments with 31or 34 days dry are shown in orange.
1130
1131
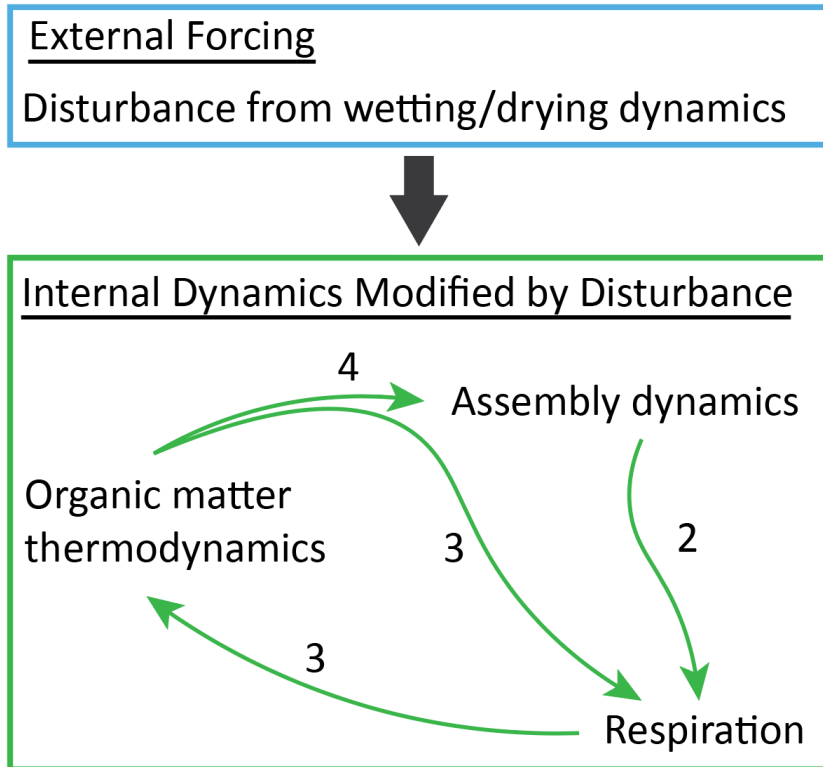
1132
1133
1134 **Figure 6. Integrated conceptual interpretation of results from this study.** Collectively, our results
1135 indicate that the external forcing imposed by disturbance leads to feedback between assembly of the
1136 putatively active community and respiration rates that is modulated by coupled dynamics in organic
1137 matter thermodynamics. Relative to Fig. 1, here external and internal aspects of the environment are
1138 separated. The arrows within the internal dynamics component are analogous to arrows 2,3, and 4 in
1139 Figure 1. The arrow from external to internal is not considered in Figure 1, and represents the impact of
1140 external forcing on all aspects of the internal system. These impacts are both direct effects of
1141 disturbance and indirect effects mediated through the internal feedback that collectively lead to impacts
1142 of re-wetting that are contingent on desiccation history.